

Review

2D Saturable Absorbers for Fibre Lasers

Robert I. Woodward * and Edmund J. R. Kelleher

Femtosecond Optics Group, Department of Physics, Imperial College London, London SW7 2BW, UK;
E-Mail: edmund.kelleher08@imperial.ac.uk

* Author to whom correspondence should be addressed; E-Mail: r.woodward12@imperial.ac.uk;
Tel.: +44-20-7594-7639.

Academic Editor: Totaro Imasaka

Received: 2 November 2015 / Accepted: 23 November 2015 / Published: 30 November 2015

Abstract: Two-dimensional (2D) nanomaterials are an emergent and promising platform for future photonic and optoelectronic applications. Here, we review recent progress demonstrating the application of 2D nanomaterials as versatile, wideband saturable absorbers for Q-switching and mode-locking fibre lasers. We focus specifically on the family of few-layer transition metal dichalcogenides, including MoS₂, MoSe₂ and WS₂.

Keywords: saturable absorbers; pulsed lasers; mode-locking; Q-switching; nanomaterials; nonlinear optical materials; graphene; MoS₂; MoSe₂; WS₂

1. Introduction

Fibre lasers are a mature technology that has become an essential tool facilitating a wide range of scientific, medical and industrial applications. The flexibility, reliability and compact nature of such light sources enables them to outperform bulk lasers in many areas: offering alignment-free, turn-key operation for end-users [1]. Pulsed operation of fibre lasers is of particular importance, leading to a significant enhancement of the instantaneous power, suitable for driving nonlinear optical processes while enabling high-resolution, time-resolved applications.

While many schemes for generating pulsed laser emission exist, passive mode-locking (*i.e.*, phase-locking of many longitudinal cavity modes) or Q-switching (*i.e.*, modulation of the laser cavity Q-factor) using a saturable absorber (SA) (a material that exhibits an intensity-dependent transmission) are often preferred, as they enable a wide space of pulse parameters to be accessed without

employing costly and complex electrically-driven modulators that ultimately impose a lower limit on the pulse durations achievable directly from the laser source [1,2].

Saturable absorbers can be broadly divided into two categories: real SAs, materials that exhibit an intrinsic nonlinear decrease in absorption with increasing light intensity; and artificial SAs, devices that exploit nonlinear effects to mimic the action of a real saturable absorber by inducing an intensity-dependent transmission. Here, we restrict the focus of our review to real SAs, considering the role of emergent 2D nanomaterials for this function and highlighting the benefits that they offer in terms of wideband operation, switching speed and engineerable properties.

Advances in saturable absorber technologies are almost synonymous with the evolution of the laser itself: the first demonstrations of SA-based pulse generation in 1964 using both a “reversibly bleachable” dye [3] and a coloured glass filter [4] to Q-switch a ruby laser were reported just four years after Maiman’s successful demonstration of laser operation [5]. In Figure 1, we highlight the historical evolution of the salient SA technologies. After these initial demonstrations, reversibly bleachable (or saturably absorbing) dyes were widely applied to mode-lock lasers, where the gain medium was also a dye, leading to the first demonstration of continuous-wave (CW) mode-locking [6].

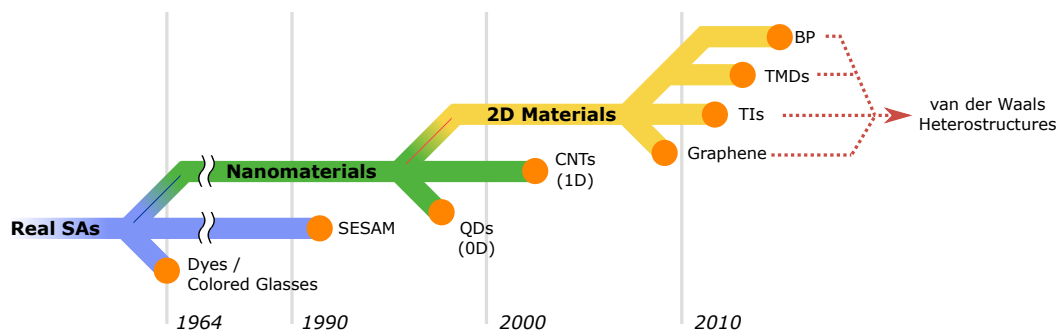


Figure 1. The evolution of real saturable absorber technologies. Orange dots denote the first reported application of each technology in a pulsed laser.

With continued development in low-loss optical fibre, mode-locked lasers based on actively-doped fibre amplifiers emerged, including an early 1983 report of unstable mode-locking of a Nd:fibre laser using a dye SA [7]. However, the passive generation of stable mode-locked pulses using an SA in fibre systems remained challenging until the semiconductor saturable absorber mirror (SESAM) was proposed in the early 1990s [8,9]. SESAMs quickly became, and remain to be, a highly successful technology for generating ultrafast mode-locked pulses and high-energy Q-switched emission from fibre lasers. However, they offer only a narrow operating bandwidth, require costly fabrication and packing, and the relaxation speed is limited to picosecond time scales (unless expensive post-processing techniques are employed) [2]. These limitations are driving research into novel materials for SA applications; of particular interest are nanomaterials, where reduced dimensionality leads to strong quantum confinement, new physical phenomena and remarkable optoelectronic properties [10,11].

While it could be argued that early reports of saturable absorption using coloured glass filters exploited nanomaterials, since the glasses were doped with semiconductor nanocrystals (*i.e.*, zero-dimensional quantum dots (QDs)), such as cadmium selenide [4], to modify their colour, it was not until 1997 that QDs were explicitly engineered for the purpose of pulse generation [12]. After

this demonstration, the field of nanomaterial SAs gained traction as 1D carbon nanotubes [13] (CNTs) and 2D graphene [14,15] emerged as promising materials exhibiting intensity-dependent absorption and sub-picosecond relaxation times [16]. Graphene, a single atomic layer of carbon atoms that can be exfoliated from graphite, attracted particular interest, as its 2D structure and zero bandgap enable wideband optical operation [10]. However, graphene is only one of a family of 2D materials that can be extracted as monolayer and few-layer crystals from a variety of bulk materials, including topological insulators (TIs), transition metal dichalcogenides (TMDs) and black phosphorous (BP). All of these materials offer distinct, yet complementary properties [10,11,17,18] and, hence, new opportunities for optical applications in fibre-based systems. The possibility of combining layers of 2D materials to form van der Waals heterostructures also offers an exciting prospect for a wide range of new engineerable photonic devices [19], as does the potential to vary nanomaterial properties through their growth conditions, doping and electronic control [20,21].

In this review, we summarize recent progress in 2D SAs, with an emphasis on few-layer transition metal dichalcogenides, a sub-class of 2D materials currently receiving particular interest. We discuss their nonlinear optical properties, which can be tuned through the fabrication procedure, and highlight recent demonstrations of Q-switched and mode-locked fibre lasers based on the technology. Finally, we conclude with an outlook exploring the opportunities and avenues for future work in this vibrant field.

2. Few-Layer Transition Metal Dichalcogenides

2.1. Fundamental Materials Science

TMDs are a group of 40+ layered materials, with the chemical structure MX_2 . The layers consist of a single plane of hexagonally-arranged transition metal (M) atoms (e.g., molybdenum, Mo, tungsten, W) covalently bonded between two hexagonal planes of chalcogen (X) atoms (e.g., sulphur, S, selenium, Se); the layers themselves are weakly bound together by van der Waals forces (Figure 2a) [22]. Semiconducting TMDs (e.g., MoS_2 , MoSe_2 , WS_2) are currently experiencing renewed interest for photonic and optoelectronic applications, expanding upon earlier studies conducted in the 1960s [22,23], with the use of modern fabrication and characterization techniques allowing new insight.

As is characteristic for 2D materials, the properties of few-layer TMDs depend on the number of layers in the material [11]. For instance, bulk MoS_2 has an indirect ~ 1.29 eV (961 nm) bandgap, which increases due to stronger quantum confinement as the number of layers is reduced, eventually becoming a direct 1.80 eV (689 nm) bandgap semiconductor in isolated monolayer form [24]. Similar behaviour is observed for other semiconducting TMDs; for example, MoSe_2 exhibits a cross-over from an indirect 1.1 eV (1128 nm) gap to a direct 1.55 eV (800 nm) gap [25], and WS_2 shows an indirect 1.4 eV (886 nm) to direct 2.1 eV (590 nm) transition [26]. An additional result of the reduced dimensionality is the emergence of strong excitonic effects.

In a semiconductor, photoexcitation places an electron into the conduction band, leaving a hole in the valence band. If the electron-hole interaction is weak (e.g., due to long-distance separation), they can each be considered as free carriers. However, their proximity can result in an attractive Coulombic interaction, creating a bound-state quasiparticle known as an exciton [27]. The photon energy required

to create a bound exciton is less than the threshold for creating free carriers. Therefore, excitons can be understood as occupying energy levels that lie below the conduction band (Figure 2b, where each excitonic transition is labelled with a letter, according to standard nomenclature [22]), although this visualization is not physically correct, as it combines a one-electron and two-particle picture [27], the hybrid scheme is widely adopted in the literature, as it provides an intuitive interpretation of the level structure. This leads to two definitions of the bandgap: the electronic bandgap (or transport gap) E_g , which defines the energy required to inject an electron-hole pair into the material, and the optical bandgap E_o , which is the lowest absorbed photon energy. The energy difference is known as the exciton binding energy: $E_b = E_g - E_o$ [28].

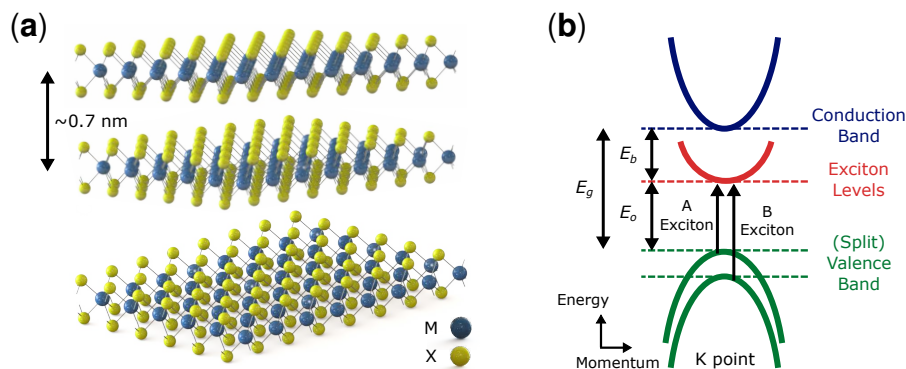


Figure 2. Transition metal dichalcogenide structure: (a) visualization of three-layer crystal; (b) simplified energy structure at crystal K point for a typical monolayer semiconducting transition metal dichalcogenide (TMD), showing the relationship between the electronic bandgap E_g , the excitonic binding energy E_b and the optical bandgap E_o , including a split valence band from spin-orbit coupling. Excitonic transitions are labelled with letters according to standard nomenclature [22].

In a typical inorganic semiconductor, the exciton binding energy is small (<10 meV) [28]. Therefore, generated excitons can rapidly ionize via collisions with optical phonons (lattice vibrations); hence, their influence is negligible at room temperature [27,28]. However, for few-layer TMDs, increased quantum confinement and reduced dielectric screening results in large excitonic binding energies (>100 meV) and strong excitonic effects [11]. In photonics, it is common to use the term bandgap to describe the optical gap. Additionally, in few-layer TMDs, spin-orbit coupling leads to a splitting of the valence band, as shown in Figure 2b, which offers potential for spintronic devices [11].

2.2. Fabrication Techniques

Many fabrication procedures exist for obtaining few-layer TMDs, which have evolved from graphene processing strategies [11,29]. These can be divided into exfoliation and growth techniques. Exfoliation involves cleaving monolayer or few-layer flakes from a bulk crystal, typically achieved mechanically (e.g., using Scotch tape), chemically (e.g., lithium-based intercalation) or through dispersal in solvents (known as liquid-phase exfoliation (LPE)). Alternatively, growth techniques, such as chemical vapour deposition (CVD), can produce high-quality, single layers of the material from carefully controlled chemical reactions between solid precursors [11].

Both LPE and CVD approaches have the potential for large-scale production, which is desirable for developing saturable absorbers and photonic devices commercially. CVD typically has a higher yield of large-area monolayer flakes of TMDs, while LPE produces smaller area, few-layer flakes. The flake size is an important parameter in determining the optical properties of a single TMD device. In fact, this flake-size-dependence of the optical properties offers a convenient method for engineering the materials inexpensively using LPE [30]. An example of an LPE-produced MoS₂ dispersion (or “ink” [31]) is shown in Figure 3a, following the processing technique presented in [32]. The MoS₂ dispersion contained a distribution of flake thicknesses (measured using atomic force microscopy (AFM), as shown in Figure 3b,c), and notably, ~50% of flakes had a 2–4-nm thickness, which corresponds to 4–5 layers, with lateral flake dimensions typically <200 nm [32].

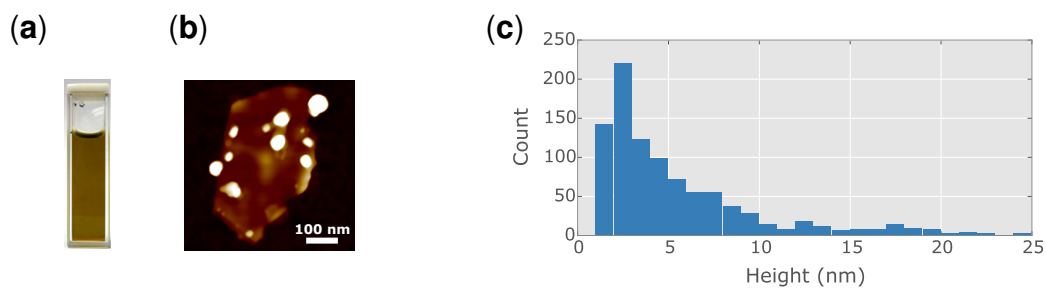


Figure 3. Fabrication of few-layer MoS₂ flakes by liquid-phase exfoliation (LPE), after [32]: (a) liquid dispersion of flakes; (b) AFM image; (c) distribution of flake heights from AFM.

To develop practical saturable absorber devices, the processed few-layer nano flakes can be integrated using a variety of optically-compatible strategies [30]. For fibre lasers applications, few-layer TMDs can be directly deposited on fibre ferrules using optical deposition or transferred to the tip of a fibre as a post-processing step [33–36]. Alternatively, they can be embedded in transparent polymer films to form compact and flexible SA devices [32,37–43]. Another attractive prospect is depositing TMD nano flakes along microfibres or D-shaped (side-polished) fibres [44–46], where the evanescent field mediates the strength of the light-matter interaction. While the light intensity on the TMD material is weaker in this case, the device interaction length can be significantly increased, which can enhance the nonlinearity, affording a higher power tolerance [44].

2.3. Nonlinear Optical Properties

2.3.1. Saturable Absorption

Effective candidate materials for SAs possess a strong intensity-dependent loss, which can be described by a two-level model:

$$\alpha(I) = \frac{\alpha_{\text{sat}}}{1 + I/I_{\text{sat}}} + \alpha_{\text{non-sat}} \tag{1}$$

where α_{sat} is the modulation depth (saturable loss), $\alpha_{\text{non-sat}}$ is the non-saturable loss and I_{sat} is the saturation intensity (required intensity to reduce the absorption by $0.5\alpha_{\text{sat}}$).

Many studies have measured the nonlinear absorption of few-layer TMD materials (e.g., using Z-scan and balanced twin-detector setups) [30]. Saturable absorption in TMDs was first revealed

by Wang *et al.*, using few-layer MoS₂ LPE dispersions containing a majority of 6–7 layer flakes: under intense 800 nm excitation, the sample transmission increased by 75%, showing a stronger nonlinear response than graphene [47]. The intraband relaxation time was also shown to be ~ 30 fs, confirming that few-layer MoS₂ can behave as an ultrafast saturable absorber [47]. These liquid dispersions were impractical for applications in fibre lasers, but inspired further nonlinear studies on fibre-compatible integration schemes.

Few-layer TMD-polymer composites have received particular attention. Using MoS₂, such devices have been fabricated and characterized at ~ 1 μm [32,44], ~ 1.5 μm [34–37,39–42,45,48] and ~ 2 μm [49] (corresponding to the gain bands for the principal active ions used in fibre lasers: ytterbium (Yb), erbium (Er) and thulium (Tm)), and a wide range of SA properties have been reported [30]. Saturable loss values have been reported from $\sim 1\%$ [40] to $\sim 11\%$ [37] with saturation intensities varying from ~ 1 MW/cm²–130 MW/cm² [42]. A persistent concern, however, is the high non-saturable losses exhibited by TMD SAs to date (often $>10\%$ [30]). While the high gain of fibre lasers can often tolerate such loss, it is desirable to reduce this value to improve device efficiency and the operation performance of pulsed fibre lasers [1].

Strong saturable absorption has also been observed in other MoS₂-based devices, such as MoS₂-coated fibre tips, where modulation depths up to 35% and saturation intensities of 0.35 MW/cm² have been reported, although this was accompanied by very high non-saturable losses of $\sim 35\%$ [34,35].

A small, but growing number of studies have produced and characterized SAs using other TMD materials, including WS₂ [42,50–54], MoSe₂ [42,55,56] and WSe₂ [42]; all have reported similar optical properties to MoS₂, including values of modulation depth and saturation intensity. Figure 4 presents the optical characterization of a polymer composite including 6–7 MoSe₂ flakes. The linear absorption profile (Figure 4a) reveals the characteristic excitonic features (labelled A and B [22]), which are a well-known feature of TMDs and can be used to identify such materials. The absorption is relatively flat, but finite, throughout the near-infrared (the origin of which is discussed later). Z-scan experiments were used to measure the intensity-dependent absorption (Figure 4b), which is well-fitted by Equation (1) to reveal the device parameters: 4.7% modulation depth, 3.4 MW/cm² saturation intensity and 6.5% non-saturable loss.

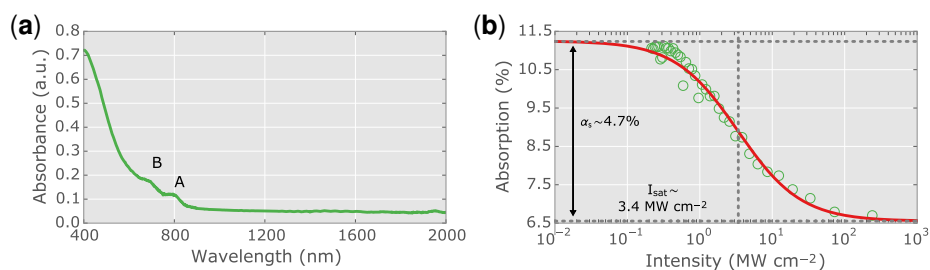


Figure 4. Characterization of MoSe₂-PVAc composite, after [55]: (a) linear absorption; (b) Z-scan measurement, fitted with a two-level saturable absorber (SA) model (solid red line) to determine device performance parameters. Labels A and B refer to excitonic transitions, as described in Section 2.1.

Due to differences in fabrication procedures and the concentrations of nano flakes in the reported SA devices to date, it is difficult to directly compare the performance from literature values; however, Chen *et al.* recently performed a comparative study under controlled fabrication conditions, showing that their MoSe₂ SA possessed a stronger modulation depth (6.7%) compared to MoS₂ (2.2%), WS₂ (2.5%) and WSe₂ (3.0%), in addition to lower non-saturable loss [42]. Further studies are required to critically evaluate the many emerging TMDs for fibre laser SA applications.

2.3.2. Origin of Sub-Bandgap Saturable Absorption

Surprisingly, many of the reports to date observing saturable absorption in few-layer TMDs have been demonstrated at near-infrared wavelengths, which corresponds to photon energies less than the expected material bandgap for most TMDs. In a perfect crystalline semiconductor, incident photons with energy lower than the bandgap would not be absorbed [27]. However, crystallographic defects, including edges and vacancies, have been proposed to explain this phenomena [32].

For the wide body of work reporting SAs based on LPE-processed TMD flakes, the flake size is often on a sub-wavelength scale, and as such, they cannot be considered as infinite crystal structures. Broken symmetry at the edges of atomic planes and unsatisfied bonds of M and X atoms at edges can modify the electronic structure, leading to the creation of edge-states in the bandgap. Given the large edge to surface area ratio of nano flakes, the contribution of edges is significant, as verified by photothermal deflection spectroscopy measurements of sub-bandgap absorption [57]. More recently, the role of defects in TMDs has been verified by theoretical studies of the band structure, showing that edges result in a finite local density of states within the bandgap of MoS₂ crystals [58]. Absorption of photons with sub-bandgap energies is thus permitted by electron transitions from the valence band to these mid-gap states, which can be saturated at high intensity by Pauli blocking [32].

A distribution of edge states within the bandgap could explain the recent experimental reports of wideband saturable absorption, although the density of states is not expected to be constant throughout the bandgap, as shown in [58], and will depend on the geometry and edge termination (whether M or X sites). Defects may also explain observations of SA at sub-bandgap photon energies in TMD flakes grown using CVD [30,34]; however, the role of edges may be less significant due to typically larger flake sizes. Other crystallographic defects, such as vacancies and grain boundaries, could contribute to sub-bandgap absorption, as verified by numerical simulations in both MoS₂ [58,59] and WS₂ [53].

2.3.3. Other Nonlinear Effects

Nonlinear optical phenomena beyond SA have also been observed in 2D TMDs. Indeed, for many nonlinear absorption studies on TMD materials, the effect was not monotonic: under sufficiently high intensity, the material exhibited an increase in absorption for increasing intensity (*i.e.*, reverse saturable absorption, RSA, or optical limiting) [33,42,54,56,60]. This RSA effect has been attributed to two-photon absorption (TPA), where under intense illumination, two photons can transfer their energy to excite a single electron over the bandgap, explaining why this effect has been observed for excitation wavelengths corresponding to photon energies less than the material bandgap, but greater than half the

gap energy. For SAs in fibre lasers, this transition from SA to RSA can influence the intra-cavity pulse dynamics and affect the transition between Q-switching and mode-locking regimes [61].

Studies have also demonstrated a dependence of the nonlinearity on the flake sizes. For example, Wang *et al.* showed that if the incident photon energy lies between the bulk bandgap and the bandgap of a monolayer for a given TMD, the flake thickness will determine whether the sample exhibits SA or TPA behaviour, since the layer count defines the energy of the bandgap [62]. Zhou *et al.* compared flakes of >100 nm, with ~ 50 nm lateral size (of constant thickness), and showed that excited state absorption (ESA) occurred in the smaller flakes. They proposed that a greater number of edge-states existed in the bandgap for smaller flakes, which were quenched at high incident intensities [60]. The ratio of edge to surface area has also been attributed to sub-bandgap saturable absorption [32]. Additionally, it was shown that thermal effects under nanosecond or longer optical pulse excitation can lead to effects, including the formation of micro-bubbles, which cause nonlinear scattering. Nonlinear scattering manifests as an optical limiting behaviour similar to RSA [33,60].

Work is ongoing to understand how the fabrication procedure and flake geometry affect the nonlinear optical properties, although it is promising that such a wide parameter space can be achieved using 2D TMDs, suggesting that SAs can be engineered to meet a wide range of requirements for different lasers.

3. Pulsed Fibre Lasers Using 2D Materials

The inclusion of a SA into a fibre laser can initiate pulsation by Q-switching or mode-locking, where the output properties depend on the cavity design and saturable absorber properties.

3.1. Q-Switched Fibre Lasers

Q-switching results from the SA modulating the cavity Q factor to periodically emit light as a pulse train, typically with a kHz repetition rate, ns– μ s pulse durations and high pulse energies (nJ–mJ level). Such lasers have become important tools in machining and materials processing [1]. Q-switched fibre lasers have been demonstrated using a variety of 2D materials, initially with graphene in 2011 [63] and subsequently with the topological insulator (TI) Bi_2Se_3 [64], TMD MoS_2 [38] and, most recently, BP [65].

Focusing on TMDs, greatest progress has been demonstrated with MoS_2 . The first MoS_2 Q-switched fibre laser was a Yb-doped fibre ring cavity, producing ~ 2.7 μ s pulses at 1068 nm with a repetition rate of 67 kHz and 0.5 mW of output power [38]. Since this initial report, further MoS_2 -based lasers have been demonstrated utilizing Yb active fibre at ~ 1 μ m [32,38,40], in addition to using Er fibre at ~ 1.5 μ m [35,36,40,41,48] and Tm fibre for ~ 2 μ m operation [40]. These results, in addition to reports of continuously tunable operation from 1030–1070 nm [32] and 1520–1568 nm [41], confirm the promising wideband saturable absorption of the material. The highest output power from MoS_2 Q-switched lasers to date is 47 mW [40], corresponding to a pulse energy of 1.2 μ J.

Q-switched lasers using other TMD materials are also emerging. For example, WS_2 [42,50,66,67] and WSe_2 [42] have been demonstrated in passively Q-switched Er:fibre lasers. Additionally, a single MoSe_2 SA was used to Q-switch Yb, Er and Tm-doped fibre lasers [55]. These MoSe_2 Q-switched lasers

all employed ring-cavity designs and generated self-starting stable pulse trains at 1060 nm, 1566 nm and 1924 nm, respectively, as shown in Figure 5.

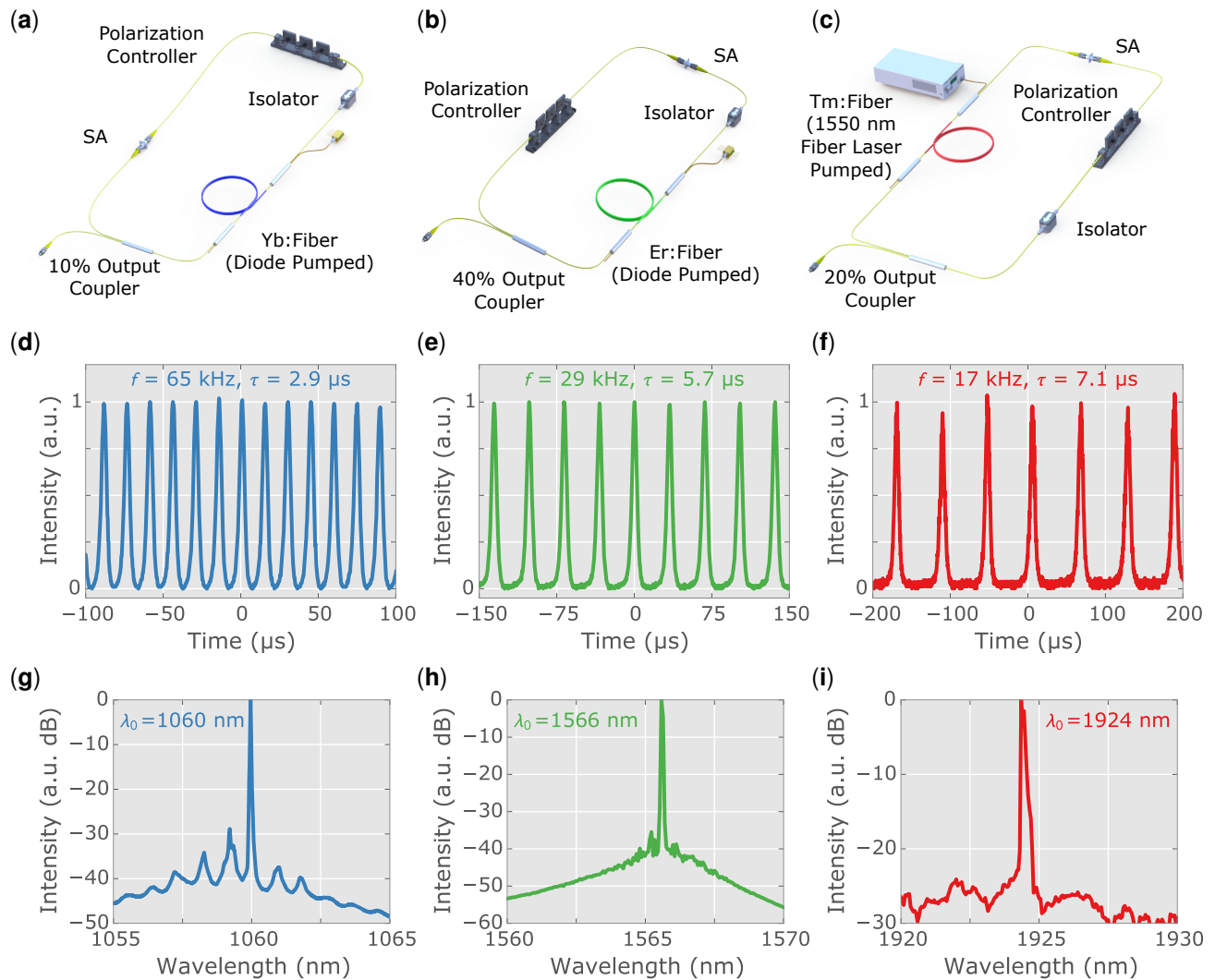


Figure 5. Q-switched fibre lasers with MoSe₂-PVA saturable absorber, after [55]: (a–c) cavity schematics; (d–f) output pulse trains showing the repetition rate f and pulse duration τ ; (g–i) spectra. The columns (left to right) show Yb, Er and Tm laser results.

3.2. Mode-Locked Fibre Lasers

Mode-locking can arise when a SA modulates the loss once per cavity round-trip, thus phase-locking the oscillating longitudinal modes, leading to the generation of a train of ultrashort (ps–fs duration) pulses at a defined repetition rate corresponding to the free spectral range of the cavity (typically MHz for few meter-long fibre lasers). Mode-locked pulse sources have a wide range of applications, notably for metrology, frequency comb generation and biophotonic imaging [1].

Typically, fibre lasers incorporating an SA can exhibit both Q-switching and mode-locking. The transition between the two regimes is mediated by a balance between gain and loss and can be controlled by the pump power; for example, the threshold for CW mode-locking is higher than that for Q-switching. However, the duration of the circulating pulse in the mode-locking regime is typically

on the order of a few ps or even hundreds of fs, such that effects arising from cavity nonlinearity and dispersion influence pulse formation. Thus, a Q-switched fibre laser may not be able to access the mode-locking regime, even at higher pump powers, without management of the cavity dispersion map and careful design of the SA device, e.g., modulation depth and reduction of the $\alpha_{\text{non-sat}}$ [1,68].

As with Q-switching, mode-locking has been demonstrated using a variety of 2D material SAs [16,30,69], with the first report in 2009 employing graphene [14,15], followed by the TIs Bi_2Te_3 [70] and Sb_2Te_3 [71], the TMD MoS_2 [33] and, recently, utilizing BP [65,72].

The first TMD mode-locked laser was reported by Zhang *et al.*, where MoS_2 was deposited on a fibre ferrule and integrated into a Yb:fibre ring cavity [33]. The laser produced 800 ps pulses at a 6.6 MHz pulse repetition frequency, with an average output power of 9.3 mW [33]. Further work through cavity dispersion engineering resulted in sub-picosecond pulse generation [39,45,66,73], down to 637 fs [45]. These ultrafast lasers operated in the net anomalous dispersion regime, generating solitons. However, recent work has shown that all-normal and net-normal dispersion maps, producing dissipative solitons, can enable higher pulse energies [1,74]. Such designs have also been exploited for TMD-based mode-locked fibre lasers [33,44,45,53].

For accessing higher repetition rates, harmonic mode-locking has been demonstrated. The highest result to date has been 2.5 GHz, mode-locking up to the 369th harmonic of a ~ 30 m cavity [46]. In terms of wavelength coverage, Yb:fibre lasers have been mode-locked using MoS_2 [33,44] and WS_2 [53], Er:fibre lasers with MoS_2 [34,39,45,46,75,76], WS_2 [52–54,66], MoSe_2 [56] and Tm:fibre lasers with MoS_2 [49] and WS_2 [51]. Continuously tunable mode-locking in the erbium gain band has also been demonstrated with a single MoS_2 -PVA composite device [37]. The laser and output characteristics shown in Figure 6 confirm the generation of stable trains of ultrashort pulses, tunable from 1535–1565 nm.

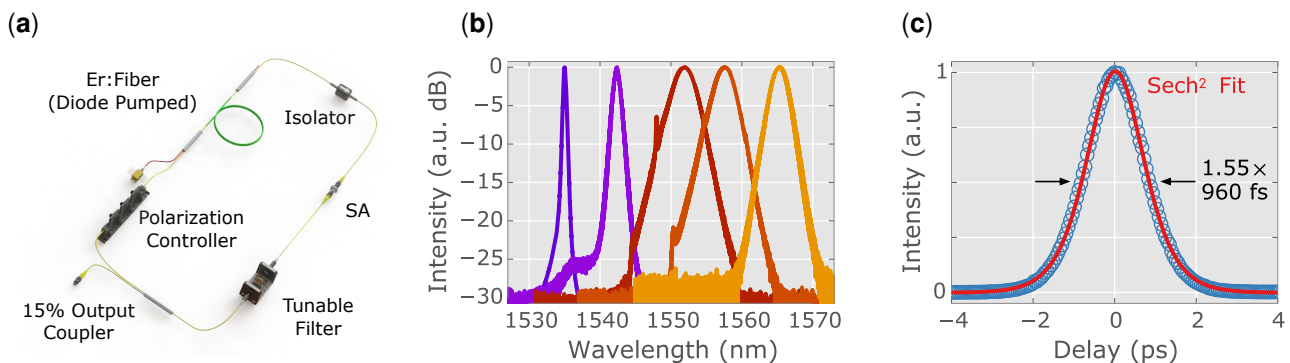


Figure 6. Tunable mode-locked Er:fibre laser using MoS_2 -PVA saturable absorber, after [37]: (a) cavity schematic; (b) examples of optical spectra from the continuous tuning range of 1535–1565 nm; (c) autocorrelation trace at 1552 nm (assuming sech^2 -shaped pulses, the deconvolution factor is 1.55).

To date, only modest output powers have been achieved in TMD-based mode-locked lasers. Typical output powers are < 10 mW [30], although notably, the highest output power reported is 150 mW from a few-layer MoS_2 mode-locked Tm:fibre laser operating in the dissipative soliton regime [49]. Amplification and power scaling will enable such laser systems to access higher powers.

4. Outlook

Significant progress has been made in the understanding of 2D materials, and their unique optical properties promise to shape the future of photonic and optoelectronic technologies [10]. In this review, we have highlighted how wideband operation and ultrafast relaxation dynamics offered by a broad array of 2D materials could play a role in enabling practical, low-cost and flexible saturable absorber devices for integrated pulsed fibre lasers.

Few-layer semiconducting TMDs are of particular interest due to their engineerable optical properties mediated by a layer-count dependent bandgap covering the visible region that transitions from indirect to direct gap behaviour for monolayers [11,24]. After initial successes demonstrating the effectiveness of MoS₂ [30] as a saturable absorber in pulsed fibre lasers, recent studies have considered other members of the TMD family of 2D materials, including MoSe₂, WS₂ and WSe₂, revealing complementary optical properties and suitability as a high-potential photonic platform. Strong intensity-dependent absorption has been measured, with the magnitude of the nonlinear optical response being found to depend on flake size and thickness, suggesting that few-layer TMD-based devices could be engineered for specific applications [60,62].

Consequently, passively Q-switched and mode-locked fibre lasers realized using TMDs have been reported throughout the near-infrared region. To date, the majority of TMD-based short-pulse laser demonstrations have operated at near-infrared wavelengths, corresponding to photon energies lower than the material bandgap for few-layer TMDs. The observed wideband saturable absorption behaviour has been explained by considering the role of crystal defects, including edge states [32]. Sources have been developed generating pulses at repetition rates from kHz–GHz, with durations from fs–μs. The maximum output powers to date have been limited to 150 mW, although this value and the parameter space of accessible pulse properties is expected to increase in the future by exploiting emerging fibre laser designs [1,77,78] and using TMD-based pulse sources to seed master-oscillator power fibre amplifier schemes [1].

One particularly promising avenue for exploiting TMD-based SAs is for the development of visible fibre lasers, where emission wavelengths can coincide with the fundamental resonances of the material; compared to graphene, this approach could offer significantly reduced saturation intensities and improved system performance. Preliminary reports have emerged using MoSe₂-based devices to Q-switch a Pr:ZBLAN fibre laser at 635 nm [79], but further work is needed to improve lasers at this wavelength and to explore the role of excitonic effects in the materials.

Beyond TMDs, few-layer TIs, with metallic edge-states, also offer potential wideband operation for photonic systems [70,71]. In addition, BP has been shown to exhibit a layer-dependent bandgap, tunable from 0.3 eV (bulk) to 2.0 eV (monolayer) [80], that could be widely exploited for both photonic and optoelectronic applications.

With the broad and increasing catalogue of available 2D materials, further studies to critically compare their performance as SAs under controlled conditions are required. An additional exciting opportunity lies in the engineering of hybrid-systems by stacking multiple single-layers to form van der Waals heterostructures [19]. Very recently, a graphene-Bi₂Te₃ heterostructure was demonstrated as a successful SA [81], prompting further work to understand the origin and scale of the nonlinear

optical response. The transfer of 2D material-based SA devices from the research laboratory to a commercially-viable technology will depend on long-term reliability and the large-scale manufacturing potential. If successful, this new platform could leverage benefits in short-pulse fibre laser technology.

Acknowledgements

We thank Roy Taylor, Tawfique Hasan, Meng Zhang, Richard Howe and Guohua Hu for fruitful discussions. Edmund Kelleher acknowledges support from the Royal Academy of Engineering.

Author Contributions

Both authors contributed to performing the literature review and writing the manuscript.

Conflicts of Interest

The authors declare no conflict of interest.

References

1. Okhotnikov, O.G. *Fibre Lasers*; Wiley: Berlin, Germany, 2012.
2. Keller, U. Recent developments in compact ultrafast lasers. *Nature* **2003**, *424*, 831–838.
3. Soffer, B.H. Giant pulse laser operation by a passive, reversibly bleachable absorber. *J. Appl. Phys.* **1964**, *35*, 2551.
4. Bret, G.; Gires, F. Giant-pulse laser and light amplifier using variable transmission coefficient glasses as light switches. *Appl. Phys. Lett.* **1964**, *4*, 175–176.
5. Maiman, T.H. Stimulated optical radiation in ruby. *Nature* **1960**, *187*, 493–494.
6. Ippen, E.P.; Shank, C.V.; Dienes, A. Passive mode locking of the cw dye laser. *Appl. Phys. Lett.* **1972**, *21*, 348–350.
7. Dzhibladze, M.I.; Esiashvili, Z.G.; Teplitskit, E.S.; Isaev, S.K.; Sagaradze, V.R. Mode locking in a fibre laser. *Sov. J. Quantum Electron.* **1983**, *13*, 245–247.
8. Zirngibl, M.; Stulz, L.W.; Stone, J.; Hugi, J.; DiGiovanni, D.J.; Hansen, P.B. 1.2 ps pulses from passively mode-locked laser diode pumped Er-doped fibre ring laser. *Electron. Lett.* **1991**, *27*, 1734–1735.
9. Keller, U.; Miller, D.A.B.; Boyd, G.D.; Chiu, T.H.; Ferguson, J.F.; Asom, M.T. Solid-state low-loss intracavity saturable absorber for Nd:YLF lasers: An antiresonant semiconductor Fabry-Perot saturable absorber. *Opt. Lett.* **1992**, *17*, 505–507.
10. Novoselov, K.S.; Jiang, D.; Schedin, F.; Booth, T.J.; Khotkevich, V.V.; Morozov, S.V.; Geim, A.K. Two-dimensional atomic crystals. *Proc. Natl. Acad. Sci. USA* **2005**, *102*, 10451–10453.
11. Wang, Q.H.; Kalantar-Zadeh, K.; Kis, A.; Coleman, J.N.; Strano, M.S. Electronics and optoelectronics of two-dimensional transition metal dichalcogenides. *Nat. Nanotechnol.* **2012**, *7*, 699–712.

12. Guerreiro, P.T.; Ten, S.; Borrelli, N.F.; Butty, J.; Jabbour, G.E.; Peyghambarian, N. PbS quantum-dot doped glasses as saturable absorbers for mode locking of a Cr: Forsterite laser. *Appl. Phys. Lett.* **1997**, *71*, 1595–1597.
13. Set, S.; Yaguchi, H.; Tanaka, Y.; Jablonski, M. Ultrafast fibre pulsed lasers incorporating carbon nanotubes. *IEEE J. Sel. Top. Quantum Electron.* **2004**, *10*, 137–146.
14. Bao, Q.; Zhang, H.; Wang, Y.; Ni, Z.; Yan, Y.; Shen, Z.X.; Loh, K.P.; Tang, D.Y. Atomic-layer graphene as a saturable absorber for ultrafast pulsed lasers. *Adv. Funct. Mater.* **2009**, *19*, 3077–3083.
15. Hasan, T.; Sun, Z.; Wang, F.; Bonaccorso, F.; Tan, P.H.; Rozhin, A.G.; Ferrari, A.C. Nanotube-polymer composites for ultrafast photonics. *Adv. Mater.* **2009**, *21*, 3874–3899.
16. Martinez, A.; Sun, Z. Nanotube and graphene saturable absorbers for fibre lasers. *Nat. Photonics* **2013**, *7*, 842–845.
17. Xia, F.; Wang, H.; Jia, Y. Rediscovering black phosphorus as an anisotropic layered material for optoelectronics and electronics. *Nat. Commun.* **2014**, *5*, doi:10.1038/ncomms5458.
18. Zhang, Y.; He, K.; Chang, C.Z.; Song, C.L.; Wang, L.L.; Chen, X.; Jia, J.F.; Fang, Z.; Dai, X.; Shan, W.Y.; *et al.* Crossover of the three-dimensional topological insulator Bi₂Te₃ to the two-dimensional limit. *Nat. Physics* **2010**, *6*, 584–588.
19. Geim, A.K.; Grigorieva, I.V. Van der Waals heterostructures. *Nature* **2013**, *499*, 419–425.
20. Lin, Y.H.; Lin, S.F.; Chi, Y.C.; Wu, C.L.; Cheng, C.H.; Tseng, W.H.; He, J.H.; Wu, C.I.; Lee, C.K.; Lin, G.R. Using n- and p-type Bi₂Te₃ topological insulator nanoparticles to enable controlled femtosecond mode-locking of fibre lasers. *ACS Photonics* **2015**, *2*, 481–490.
21. Lee, E.J.; Choi, S.Y.; Jeong, H.; Park, N.H.; Yim, W.; Kim, M.H.; Park, J.K.; Son, S.; Bae, S.; Kim, S.J.; *et al.* Active control of all-fibre graphene devices with electrical gating. *Nat. Commun.* **2015**, *6*, doi:10.1038/ncomms7851.
22. Wilson, J.A.; Yoffe, A. The transition metal dichalcogenides: Discussion and interpretation of the observed optical, electrical and structural properties. *Adv. Phys.* **1969**, *18*, 193–335.
23. Frindt, R.F. Optical absorption of a few unit-cell layers of MoS₂. *Phys. Rev.* **1965**, *140*, A536–A539.
24. Mak, K.F.; Lee, C.; Hone, J.; Shan, J.; Heinz, T.F. Atomically thin MoS₂: A new direct-gap semiconductor. *Phys. Rev. Lett.* **2010**, *105*, 136805–136811.
25. Tongay, S.; Zhou, J.; Ataca, C.; Lo, K.; Matthews, T.S.; Li, J.; Grossman, J.C.; Wu, J. Thermally driven crossover from indirect toward direct bandgap in 2D semiconductors: MoSe₂ versus MoS₂. *Nano Lett.* **2012**, *12*, 5576–5580.
26. Kuc, A.; Zibouche, N.; Heine, T. Influence of quantum confinement on the electronic structure of the transition metal sulfide TS₂. *Phys. Rev. B* **2011**, *83*, doi:10.1103/PhysRevB.83.245213.
27. Yu, P.Y.; Cardona, M. *Fundamentals of Semiconductors: Physics and Materials Properties*; Springer: Berlin, Germany, 2010.
28. Kasap, S.; Capper, P. *Springer Handbook of Electronic and Photonic Materials*; Springer: Berlin, Germany, 2006.
29. Bonaccorso, F.; Lombardo, A.; Hasan, T.; Sun, Z.; Colombo, L.; Ferrari, A.C. Production and processing of graphene and 2D crystals. *Mater. Today* **2012**, *15*, 564–589.

30. Woodward, R.I.; Howe, R.C.T.; Hu, G.; Torrisi, F.; Zhang, M.; Hasan, T.; Kelleher, E.J.R. Few-layer MoS₂ saturable absorbers for short-pulse laser technology: current status and future perspectives [Invited]. *Photonics Res.* **2015**, *3*, A30–A42.
31. Howe, R.C.T.; Hu, G.; Yang, Z.; Hasan, T. Functional inks of graphene, metal dichalcogenides and black phosphorus for photonics and (opto)electronics. In Proceeding of Low-Dimensional Materials and Devices, San Diego, CA, USA, 9 August 2015.
32. Woodward, R.I.; Kelleher, E.J.R.; Howe, R.C.T.; Hu, G.; Torrisi, F.; Hasan, T.; Popov, S.V.; Taylor, J.R. Tunable Q-switched fibre laser based on saturable edge-state absorption in few-layer molybdenum disulfide (MoS₂). *Opt. Express* **2014**, *22*, 31113–31122.
33. Zhang, H.; Lu, S.B.; Zheng, J.; Du, J.; Wen, S.C.; Tang, D.Y.; Loh, K.P. Molybdenum disulfide (MoS₂) as a broadband saturable absorber for ultra-fast photonics. *Opt. Express* **2014**, *22*, 7249–7260.
34. Xia, H.; Li, H.; Lan, C.; Li, C.; Zhang, X.; Zhang, S.; Liu, Y. Ultrafast erbium-doped fibre laser mode-locked by a CVD-grown molybdenum disulfide (MoS₂) saturable absorber. *Opt. Express* **2014**, *22*, 17341–17348.
35. Li, H.; Xia, H.; Lan, C.; Li, C.; Zhang, X.; Li, J.; Liu, Y. Passively Q-switched erbium-doped fibre laser based on few-layer MoS₂ saturable absorber. *IEEE Photonics Technol. Lett.* **2015**, *27*, 69–72.
36. Khazaeinezhad, R.; Kassani, S.H.; Nazari, T.; Jeong, H.; Kim, J.; Choi, K.; Lee, J.U.; Kim, J.H.; Cheong, H.; Yeom, D.I.; *et al.* Saturable optical absorption in MoS₂ nano-sheet optically deposited on the optical fibre facet. *Opt. Commun.* **2015**, *335*, 224–230.
37. Zhang, M.; Howe, R.C.T.; Woodward, R.I.; Kelleher, E.J.R.; Torrisi, F.; Hu, G.; Popov, S.V.; Taylor, J.R.; Hasan, T. Solution processed MoS₂-PVA composite for sub-bandgap mode-locking of a wideband tunable ultrafast Er:fibre laser. *Nano Res.* **2015**, *8*, 1522–1534.
38. Woodward, R.I.; Kelleher, E.J.R.; Runcorn, T.H.; Popov, S.V.; Torrisi, F.; Howe, R.C.T.; Hasan, T. Q-switched fibre laser with MoS₂ saturable absorber. In *CLEO:2014, OSA Technical Digest*; Optical Society of America: San Jose, CA, USA, 2014; p. SM3H.6.
39. Liu, H.; Luo, A.P.; Wang, F.Z.; Tang, R.; Liu, M.; Luo, Z.C.; Xu, W.C.; Zhao, C.J.; Zhang, H. Femtosecond pulse erbium-doped fibre laser by a few-layer MoS₂ saturable absorber. *Opt. Lett.* **2014**, *39*, 4591–4594.
40. Luo, Z.; Huang, Y.; Zhong, M.; Li, Y.; Wu, J.; Xu, B.; Xu, H.; Cai, Z.; Peng, J.; Weng, J. 1-, 1.5-, and 2- μ m fibre lasers Q-switched by a broadband few-layer MoS₂ saturable absorber. *J. Lightwave Technol.* **2014**, *32*, 4679–4686.
41. Huang, Y.; Luo, Z.; Li, Y.; Zhong, M.; Xu, B.; Che, K.; Xu, H.; Cai, Z.; Peng, J.; Weng, J. Widely-tunable, passively Q-switched erbium-doped fibre laser with few-layer MoS₂ saturable absorber. *Opt. Express* **2014**, *22*, 25258–25266.
42. Chen, B.; Zhang, X.; Wu, K.; Wang, H.; Wang, J.; Chen, J. Q-switched fibre laser based on transition metal dichalcogenides MoS₂, MoSe₂, WS₂, and WSe₂. *Opt. Express* **2015**, *23*, 26723–26737.

43. Howe, R.C.T.; Woodward, R.I.; Hu, G.; Yang, Z.; Kelleher, E.J.R.; Hasan, T. Surfactant-aided exfoliation of molybdenum disulphide for ultrafast pulse generation through edge-state saturable absorption. Available online: <http://arxiv.org/abs/1508.01631> (accessed on 26 November 2015).
44. Du, J.; Wang, Q.; Jiang, G.; Xu, C.; Zhao, C.; Xiang, Y.; Chen, Y.; Wen, S.; Zhang, H. Ytterbium-doped fibre laser passively mode locked by few-layer molybdenum disulfide (MoS_2) saturable absorber functioned with evanescent field interaction. *Sci. Rep.* **2014**, *4*, doi:10.1038/srep06346.
45. Khazaeizhad, R.; Kassani, S.H.; Jeong, H.; Yeom, D.I.; Oh, K. Mode-locking of Er-doped fibre laser using a multilayer MoS_2 thin film as a saturable absorber in both anomalous and normal dispersion regimes. *Opt. Express* **2014**, *22*, 23732–23742.
46. Liu, M.; Zheng, X.W.; Qi, Y.L.; Liu, H.; Luo, A.P.; Luo, Z.C.; Xu, W.C.; Zhao, C.J.; Zhang, H. Microfibre-based few-layer MoS_2 saturable absorber for 2.5 GHz passively harmonic mode-locked fibre laser. *Opt. Express* **2014**, *22*, 22841–22846.
47. Wang, K.; Wang, J.; Fan, J.; Lotya, M.; O'Neill, A.; Fox, D.; Feng, Y.; Zhang, X.; Jiang, B.; Zhao, Q.; *et al.* Ultrafast saturable absorption of two-dimensional MoS_2 nanosheets. *ACS Nano* **2013**, *7*, 9260–9267.
48. Ren, J.; Wang, S.; Cheng, Z.; Yu, H.; Zhang, H.; Mei, L.; Wang, P. Passively Q-switched nanosecond erbium-doped fibre laser with MoS_2 saturable absorber. *Opt. Express* **2015**, *23*, 29516–29522.
49. Tian, Z.; Wu, K.; Kong, L.; Yang, N.; Wang, Y.; Chen, R.; Hu, W.; Xu, J.; Tang, Y. Mode-locked thulium fibre laser with MoS_2 . *Laser Physics Lett.* **2015**, *12*, doi:10.1088/1612-2011/12/6/065104.
50. Zhang, M.; Hu, G.; Hu, G.; Howe, R.C.T.; Chen, L.; Zheng, Z.; Hasan, T. Yb- and Er-doped fibre laser Q-Switched with an optically uniform, broadband WS_2 saturable absorber. Available online: <http://arxiv.org/abs/1507.03188> (accessed on 26 November 2015).
51. Jung, M.; Lee, J.; Park, J.; Koo, J.; Jhon, Y.M.; Lee, H. Mode-locked, 1.94- μm , all-fibreized laser using WS_2 -based evanescent field interaction. *Opt. Express* **2015**, *23*, 241–243.
52. Mao, D.; Wang, Y.; Ma, C.; Han, L.; Jiang, B.; Gan, X.; Hua, S.; Zhang, W.; Mei, T.; Zhao, J. WS_2 mode-locked ultrafast fibre laser. *Sci. Rep.* **2015**, *5*, doi:10.1038/srep07965.
53. Mao, D.; Zhang, S.; Wang, Y.; Gan, X.; Zhang, W.; Mei, T.; Wang, Y.; Wang, Y.; Zeng, H.; Zhao, J. WS_2 saturable absorber for dissipative soliton mode locking at 1.06 and 1.55 μm . *Opt. Express* **2015**, *23*, 27509–27519.
54. Yan, P.; Liu, A.; Chen, Y.; Chen, H.; Ruan, S.; Chen, S.; Li, I.L.; Yang, H.; Hu, J.; Cao, G. Microfibre-based WS_2 -film saturable absorber for ultra-fast photonics. *Opt. Mater. Express* **2015**, *5*, 479–489.
55. Woodward, R.I.; Howe, R.C.T.; Runcorn, T.H.; Hu, G.; Torrisi, F.; Kelleher, E.J.R.; Hasan, T. Wideband saturable absorption in few-layer molybdenum diselenide (MoSe_2) for Q-switching Yb-, Er- and Tm-doped fibre lasers. *Opt. Express* **2015**, *23*, 1–11.
56. Luo, Z.; Li, Y.; Zhong, M.; Huang, Y.; Wan, X.; Peng, J.; Weng, J. Nonlinear optical absorption of few-layer molybdenum diselenide (MoSe_2) for passively mode-locked soliton fibre laser [Invited]. *Photonics Res.* **2015**, *3*, A79–A86.

57. Roxlo, C.B.; Daage, M.; Rupper, A.F.; Chianelli, R.R. Optical absorption and catalytic activity of molybdenum sulfide edge surfaces. *J. Catal.* **1986**, *100*, 176–184.
58. Zhou, W.; Zou, X.; Najmaei, S.; Liu, Z.; Shi, Y.; Kong, J.; Lou, J.; Ajayan, P.M.; Yakobson, B.I.; Idrobo, J.C. Intrinsic structural defects in monolayer molybdenum disulfide. *Nano Lett.* **2013**, *13*, 2615–2622.
59. Wang, S.; Yu, H.; Zhang, H.; Wang, A.; Zhao, M.; Chen, Y.; Mei, L.; Wang, J. Broadband few-layer MoS₂ saturable absorbers. *Adv. Mater.* **2014**, *26*, 3538–3544.
60. Zhou, K.G.; Zhao, M.; Chang, M.J.; Wang, Q.; Wu, X.Z.; Song, Y.; Zhang, H.L. Size-dependent nonlinear optical properties of atomically thin transition metal dichalcogenide nanosheets. *Small* **2015**, *11*, 694–701.
61. Thoen, E.R.; Koontz, E.M.; Joschko, M.; Langlois, P.; Schibli, T.R.; Kaertner, F.X.; Ippen, E.P.; Kolodziejski, L.A. Two-photon absorption in semiconductor saturable absorber mirrors. *Appl. Phys. Lett.* **1999**, *74*, 3927–3929.
62. Wang, K.; Feng, Y.; Chang, C.; Zhan, J.; Wang, C.; Zhao, Q.; Coleman, J.N.; Zhang, L.; Blau, W.; Wang, J. Broadband ultrafast nonlinear absorption and nonlinear refraction of layered molybdenum dichalcogenide semiconductors. *Nanoscale* **2014**, *6*, 10530–10535.
63. Popa, D.; Sun, Z.; Hasan, T.; Torrisi, F.; Wang, F.; Ferrari, A.C. Graphene Q-switched, tunable fibre laser. *Appl. Phys. Lett.* **2011**, *98*, 1–3.
64. Chen, M.; Meng, Z.; Tu, X.; Zhou, H. Low-noise, single-frequency, single-polarization Brillouin/erbium fibre laser. *Opt. Lett.* **2013**, *38*, 2041–2043.
65. Chen, Y.; Jiang, G.; Chen, S.; Guo, Z.; Yu, X.; Zhao, C.; Zhang, H.; Bao, Q.; Wen, S.; Tang, D.; *et al.* Mechanically exfoliated black phosphorus as a new saturable absorber for both Q-switching and Mode-locking laser operation. *Opt. Express* **2015**, *23*, 12823–12833.
66. Wu, K.; Zhang, X.; Wang, J.; Li, X.; Chen, J. WS₂ as a saturable absorber for ultrafast photonic applications of mode-locked and Q-switched lasers. *Opt. Express* **2015**, *23*, 11453–11461.
67. Kassani, S.H.; Khazaeizhad, R.; Jeong, H.; Nazari, T.; Yeom, D.I.; Oh, K. All-fibre Er-doped Q-Switched laser based on Tungsten Disulfide saturable absorber. *Opt. Mater. Express* **2015**, *5*, 373–379.
68. Svelto, O. *Principles of Lasers*; Springer: Berlin, Germany, 2010.
69. Sobon, G. Mode-locking of fibre lasers using novel two-dimensional nanomaterials: Graphene and topological insulators [Invited]. *Photonics Res.* **2015**, *3*, A56–A63.
70. Zhao, C.; Zhang, H.; Qi, X.; Chen, Y.; Wang, Z.; Wen, S.; Tang, D. Ultra-short pulse generation by a topological insulator based saturable absorber. *Appl. Phys. Lett.* **2012**, *101*, doi:10.1063/1.4767919.
71. Sotor, J.; Sobon, G.; Macherzynski, W.; Paletko, P.; Grodecki, K.; Abramski, K.M. Mode-locking in Er-doped fibre laser based on mechanically exfoliated Sb₂Te₃ saturable absorber. *Opt. Mater. Express* **2014**, *4*, 1–6.
72. Sotor, J.; Sobon, G.; Macherzynski, W.; Paletko, P.; Abramski, K.M. Black phosphorus—A new saturable absorber material for ultrashort pulse generation. Available online: <http://arxiv.org/ftp/arxiv/papers/1504/1504.04731.pdf> (accessed on 26 November 2015).

73. Wu, K.; Zhang, X.; Wang, J.; Chen, J. 463-MHz fundamental mode-locked fibre laser based on few-layer MoS₂ saturable absorber. *Opt. Lett.* **2015**, *40*, 1374–1377.
74. Chong, A.; Buckley, J.; Renninger, W.; Wise, F. All-normal-dispersion femtosecond fibre laser. *Opt. Express* **2006**, *14*, 10095–10100.
75. Zhang, W.; Chuu, C.P.; Huang, J.K.; Chen, C.H.; Tsai, M.L.; Chang, Y.H.; Liang, C.T.; Chen, Y.Z.; Chueh, Y.L.; He, J.H.; *et al.* Ultrahigh-gain photodetectors based on atomically thin graphene-MoS₂ heterostructures. *Sci. Rep.* **2014**, *4*, doi:10.1038/srep03826.
76. Wang, Y.; Mao, D.; Gan, X.; Han, L.; Ma, C.; Xi, T.; Zhang, Y.; Shang, W.; Hua, S.; Zhao, J. Harmonic mode locking of bound-state solitons fibre laser based on MoS₂ saturable absorber. *Opt. Express* **2015**, *23*, 205–210.
77. Lefrançois, S.; Kieu, K.; Deng, Y.; Kafka, J.D.; Wise, F.W. Scaling of dissipative soliton fibre lasers to megawatt peak powers by use of large-area photonic crystal fibre. *Opt. Lett.* **2010**, *35*, 1569–1571.
78. Woodward, R.I.; Kelleher, E.J.R.; Runcorn, T.H.; Loranger, S.; Popa, D.; Wittwer, V.J.; Ferrari, A.C.; Popov, S.V.; Kashyap, R.; Taylor, J.R. Fibre grating compression of giant-chirped nanosecond pulses from an ultra-long nanotube mode-locked fibre laser. *Opt. Lett.* **2015**, *40*, 387–390.
79. Wu, D.; Peng, J.; Zhong, Y.; Cheng, Y.; Qu, B.; Weng, J.; Luo, Z.; Xu, B.; Cheng, N.; Xu, H.; *et al.* 2-D materials-based passively Q-switched 635 nm Pr³⁺-doped ZBLAN fibre lasers. In Proceedings of Advanced Solid State Lasers Conference, Berlin, Germany, 4–9 October 2015; p. ATu2A.28.
80. Tran, V.; Soklaski, R.; Liang, Y.; Yang, L. Layer-controlled band gap and anisotropic excitons in few-layer black phosphorus. *Phys. Rev. B* **2014**, *89*, doi:10.1103/PhysRevB.89.235319.
81. Mu, H.; Wang, Z.; Yuan, J.; Xiao, S.; Chen, C.; Chen, Y.; Chen, Y.; Song, J.; Wang, Y.; Xue, Y.; *et al.* Graphene-Bi₂Te₃ heterostructure as saturable absorber for short pulse generation. *ACS Photonics* **2015**, *2*, 832–841.